Electric Power Systems Research 117 (2014) 172–184

Contents lists available at ScienceDirect

Electric Power Systems Research

journal homepage: www.elsevier.com/locate/epsr

Parameterization of robust three-term power system stabilizers

M. Soliman*

Department of Electrical Power and Machines, Benha University, Cairo, Egypt

ARTICLE INFO

Article history:
Received 3 September 2013
Received in revised form 3 July 2014
Accepted 15 August 2014
Available online 11 September 2014

Keywords:
Dynamic stability
PSS design
PID control
Phase-lead compensator
Robustness
Kharitonov's theorem

ABSTRACT

This paper addresses the problem of determining robust three-term output-feedback power system stabilizers (PSSs) ($C_1(s)=(x_1s+x_2+x_3/s)$; $C_2(s)=x_1(1+x_2s)/(1+x_3s)$) which can function properly over wide range of operating conditions. Necessary and sufficient constraints that characterize the admissible set of PSSs parameters are derived firstly by applying Routh-Hurwitz (RH) criterion to the characteristic polynomial of the generalized plant model. The complete set of stabilizing PSSs for any operating point is therefore determined in the controller parameter space $[x_1, x_2, x_3]$ by plotting RH constraints at this point. Since the design parameters are load-dependent and have to be adjusted at each operating condition, an interval plant is developed to describe uncertainties in the model parameters imposed by continuous variation in load patterns. Necessary and sufficient constraints for Hurwitz stability of such interval plant are derived using Kharitonov's theorem where robust PSS design is reduced to simultaneous stabilization of finite number of vertex/segment plants. The stability region for each of these plants is plotted using RH constraints where the intersection of the resulting stability regions yields the set of parameters that guarantee Hurwitz stability of the considered interval plant. Simulation results of an applicant PSS confirm the effectiveness of the proposed design approach.

1. Introduction

Power systems are often subjected to disturbances by several reasons such as continuous load changes, set-point changes, and faults. Consequently, it exhibit low frequency oscillations that either decay gradually, or continue to grow, causing system separation. These low frequency oscillations are due to the lack of damping of the electromechanical mode of the system [1–4]. The desired additional damping can be provided by supplementary excitation control through a power system stabilizer (PSS). The main problem encountered in the conventional PSS design is that power systems constantly experience changes in operating conditions due to variations in generation and load patterns. So, a conventionally designed PSS may fail to maintain stability over wide range of operating points. Further, the performance of conventional PSS is degraded once the deviation from the nominal point becomes significant. To cope with uncertainties, imposed by continuous variation in operating points, has become the priority of the PSS designers. To make the performance of a PSS robust, the design algorithm must account for power system uncertainties. Uncertainties in the power system model can be unstructured in the form of norm-bounded parameter uncertainty [5,6], or structured associated with loading and other varying operating conditions [7–11]. Various approximations have been utilized in the modeling of uncertain systems including μ-synthesis [7–11], Lyapunov state-space based procedures [12–15], and interval polynomial [16–20]. These approaches target two main objectives; the first considers the evaluation of system robustness under the effect of parametric uncertainties, while the second considers the synthesis of PSSs that can guarantee robustness under parametric uncertainties. In Refs. [7,8], Djukanovic et al. have successfully applied the structured singular value (SSV) theory to determine robust stability of a power system for a wide range of operating conditions. A systematic procedure for sequential design of decentralized controllers, in multimachine power system, was studied in Ref. [9] where the robust performance in terms of the structured singular value (SSV or μ) was used as the measure of control performance. Castellanos et al. [10,11] have examined the application of SSV theory to the problem of evaluating the robust stability of large power systems with structured uncertainties where variations in system operating conditions and system topology are modeled as structured uncertainties and included in the nominal power system model. Rao et al. [12] reduced the controller synthesis to solve a nonlinear optimization problem where parametric uncertainty was handled using Quantitative Feedback

* Corresponding author at: Electrical Power and Machines Department, Faculty of Engineering, Benha University, 108 Shoubra St., P.O. Box 11241, Cairo, Egypt. Tel.: +20 10 05419184/2 42196348; fax: +20 2 22022310.
E-mail addresses: msoliman_28@yahoo.com, msoliman1512@gmail.com

http://dx.doi.org/10.1016/j.epsr.2014.08.013
0378-7796/

Nomenclature

All quantities are in per-unit unless otherwise stated

T_m	mechanical torque
T_e	electrical torque
V_T	terminal voltage
E'_q	voltage behind transient reactance
E_{fd}	field voltage
X'_d	generator *d*-axis transient reactance
X_d, X_q	direct axis and quadrature axis synchronous reactance
R_e, X_e	tie line resistance and reactance, respectively
δ	torque angle (rad)
K_E, T_E	exciter gain and time constant
P_g, Q_g	active and reactive power at generator bus
V^∞	infinite bus voltage
U_{pss}	stabilizing signal (PSS output)
M	inertia constant (s)
$k_1, \ldots, k_6$	parameters of the power system block-diagram
T'_{do}	open circuit *d-axis* time constant
ω_o	synchronous speed (rad/s)
$\Delta\omega$	rotor speed deviation
s	laplace operator
k_p, k_i, k_d	PID controller gains
K, T_1, T_2	parameters of a phase-lead compensator
$\underline{x}, \bar{x}$	lower and upper bounds of a variable x, respectively
$K^1, K^2, \ldots, K^4$	Kharitonov vertex polynomials
NS_i, $i = 1, \ldots, 4$	Kharitonov segments associated with $N_i(s)$, $i = 1,2, \ldots, 4$.
$G_s(s)$	family of Kharitonov segment plants
Δ_{ij}	polynomial characterizing the segment plant $G_{ij}(s, \lambda)$
$C(s)$	controller transfer function (TF)
$R_{31}, R_{21}, R_{11}, R_{01}$	Hurwitz residues for s^3, s^2, s^1, and s^0 rows
k_p^*, k_i^*	pre-specified values of k_p and k_i
k_i^{cr}, k_d^{cr}	critical values of the PID controller's parameters k_i and k_d.
$\varnothing$	empty set
ζ	damping ratio

Theory (QFT). In Ref. [13], the design of a robust decentralized state feedback PSSs was considered to guarantee pole-placement in a pre-specified region in the left-half of the complex plane. The design assumed full state measurability and considered polytopic uncertainty. Werner et al. [14] expressed the uncertainties due to variable operating points using Linear Fractional Transformation (LFT) and then an LMI technique is applied to find a 4th order H_∞ controller under regional pole placement constraints. Soliman et al. [15] suggested an iterative LMI algorithm to design robust decentralized PID based PSSs. In Ref. [16], Soliman suggested an interval arithmetic approach for computing the admissible set of robust proportional-derivative (PD) based PSS using interval Routh-Hurwitz arrays. The authors of Ref. [17] applied a generalized Kharitonov's theorem to parameter perturbations in the state space model of the power system with a PSS. The parameters of the PSS were considered as candidates for perturbations and the region of stability was computed using the edge theorem and the segment lemma. The design was carried out at certain operating point where only uncertainties in controller parameters are reported. In Ref. [18], uncertainties due to continuous variation in the operating point, was described by an interval polynomial. The design of a phase-lead PSS was reduced to simultaneous stabilization of eight vertex plants derived using Kharitonov's theorem. Root-locus technique was applied to compute only the gain where compensator's zero and pole time constants were pre-specified to ensure fast response. Rigatos and Saino [19] extended the results of Ref. [18] and presented the two-stage stabilizer. However, time constants of the compensator's poles and zeros were also pre-specified. Soliman et al. [20] presented a reconfigurable design of fault-tolerant PSS and FACTs controllers using Kharitonov's theorem where system uncertainties were represented by an interval polynomial. The gains of the controllers are computed using particle swarm optimization (PSO). The authors suggested an eigenvalue-based cost function that ensures a specific settling time. Computing the admissible set of robust phase-lead compensator's parameters, which can stabilize the plant under wide range of operating conditions, was not targeted in Refs. [17–20]. Furthermore, the case of PID based PSSs was not dealt with. In Refs. [21,22], robust PSS synthesis is reduced to a simultaneous stabilization of some operating points and then evolutionary algorithms such as genetic algorithms and particle swarm are applied to compute controller parameters while minimizing eigenvalue-based objective functions. Concisely, robust PSS design involves three basic issues regarding uncertainty modeling, controller order and solution algorithm. Robust PSS design techniques often result in a unique controller without considering the set of all admissible PSSs. Computing the set of admissible parameters gives great flexibility while implementing PSSs.

This paper presents a step to attack this problem by characterizing such set for a single-machine infinite-bus system. The robustness issue is treated using generalized Kharitonov theorem, while stability conditions derived with Routh-Hurwitz criterion are used to parameterize the stabilizing controllers. Two approaches are proposed for designing robust PID-based PSSs. The first one considers simultaneous stabilization of four segment plants while the second approach considers simultaneous stabilization of sixteen vertex plants. For phase-lead compensator design, simultaneous stabilization of only eight vertex plants is considered. The rest of the paper is organized as follows. Section 2 considers the challenge facing the design of PSSs and develops an interval plant model to capture all uncertainties imposed by loading conditions. Necessary and sufficient conditions for stabilizing an interval plant via a three-term controller using generalized Kharitonov theorem are briefly reviewed in Section 3. Parameterization of the robust PID-based PSS and that of robust phase-lead PSSs are presented in Sections 4 and 5, respectively. Section 6 presents the results while Section 7 concludes this work.

2. Problem formulation

The system under study comprises a single-machine connected to an infinite bus through a tie-line. Such system is commonly used in the analysis and design of a PSS. The system is represented by a fourth order linearized model as proposed by deMello and Concordia [3]. The linearized model of this system can be described by the block diagram shown in Fig. 1. The system data and nonlinear model are given in Appendix A.1. The model parameters k_1, k_2, k_4, k_5, k_6 shown in Fig. 1 depend basically on the values of *P and Q* while k_3 depends on the tie-line reactance only. These parameters could be expressed as explicit functions of P and Q as given in Ref. [18]. The state space realization of the system is given as follows:

$$\dot{x} = A(k)x + Bu, \quad y = Cx \tag{1}$$

where $x \in R^{4\times 1}$ is the state vector defined by $x = [\,\Delta\delta \;\; \Delta\omega \;\; \Delta E'_q \;\; \Delta E_{fd}\,]^T$, u is the stabilizing signal and the output y is typically represented by the angular speed deviation

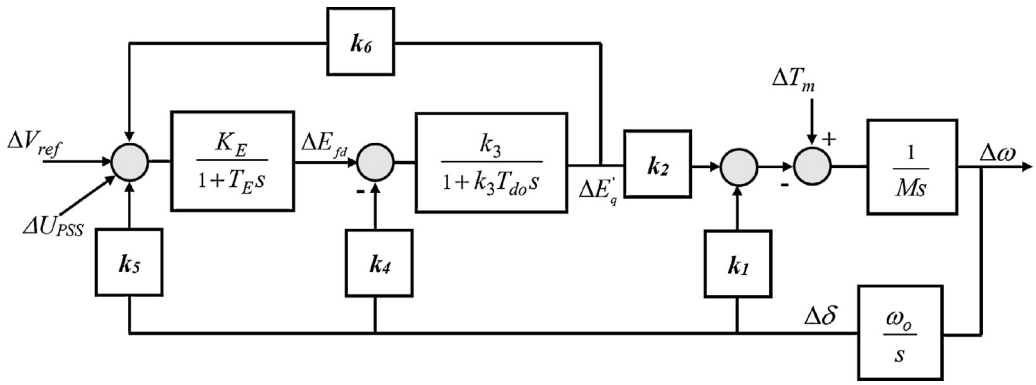

Fig. 1. Block diagram of the linearized model [1].

$\Delta\omega$. The state space matrices are defined as follows:

$$A(k)=\begin{bmatrix} 0 & \omega_o & 0 & 0 \\ -\frac{k_1}{M} & 0 & -\frac{k_2}{M} & 0 \\ -\frac{-k_4}{T'_{do}} & 0 & \frac{-1}{T'_{do}k_3} & \frac{1}{T'_{do}} \\ -\frac{K_E k_5}{T_E} & 0 & -\frac{K_E k_6}{T_E} & -\frac{1}{T'_E} \end{bmatrix},$$

$$B\begin{bmatrix} 0 & 0 & 0 & \frac{K_E}{T_E} \end{bmatrix}^T, \quad C=[0 \quad 1 \quad 0 \quad 0], \quad D=[0] \tag{2}$$

Therefore, the open loop transfer function (TF) of the system shown in Fig. 1, is given by $G_p(s)=\Delta\omega(s)/\Delta U_{pss}(s)=C(sI-A(k))^{-1}B$. Remarkably, the TF is in turn load-dependent. This TF could be evaluated at any operating point by the following general form:

$$G_p(s)=\frac{-b_1 s}{a_4 s^4+a_3 s^3+a_2 s^2+a_1 s+a_0}=\frac{-N(s)}{D(s)} \tag{3}$$

The mathematical expressions that compute the values of a_4, a_3, a_2, a_1, a_0, and b_1 as function of the machine loading and machine parameters are given in Appendix A.2. The coefficients a_4, a_3 are always constant and independent of the machine loading. The values of the coefficients a_0, a_1, a_2 and b_1 vary according to a vector κ which consists of two independent quantities (*machine loading P and Q*), i.e. $\kappa=[P \quad Q]^T$. In this study, it is assumed that $P\in[\underline{P} \quad \bar{P}]$ and $Q\in[\underline{Q} \quad \bar{Q}]$ and hence the vector κ takes values in a rectangle, in the P–Q plane, whose vertices are $(\underline{P},\underline{Q})$, $(\underline{P},\bar{Q})$, $(\bar{P},\underline{Q})$, $(\bar{P},\bar{Q})$. Consequently, any change in P and/or Q leads to corresponding changes in $a_0(\kappa)$, $a_1(\kappa)$, $a_2(\kappa)$ and $b_1(\kappa)$. Therefore, Eq. (3) describes a family of plants rather than a nominal plant as P and Q vary over their prescribed intervals. Furthermore, because $a_0(\kappa)$, $a_1(\kappa)$, $a_2(\kappa)$ and $b_1(\kappa)$ depend simultaneously on κ, this family of plants can be approximated by the following interval plant:

$$G_p(s)=\frac{-[\underline{b}_1 \quad \bar{b}_1]s}{[\underline{a}_4 \quad \bar{a}_4]s^4+[\underline{a}_3 \quad \bar{a}_3]s^3+[\underline{a}_2 \quad \bar{a}_2]s^2+[\underline{a}_1 \quad \bar{a}_1]s+[\underline{a}_0 \quad \bar{a}_0]}=\frac{-N^I(s)}{D^I(s)} \tag{4}$$

where the bounds of each interval is computed over $P\in[\underline{P} \quad \bar{P}]$ and $Q\in[\underline{Q} \quad \bar{Q}]$ as follows:

$$[\underline{a}_i \quad \bar{a}_i]=[\min_{\substack{P\in[\underline{P} \quad \bar{P}],\\ Q\in[\underline{Q} \quad \bar{Q}]}} a_i \quad \max_{\substack{P\in[\underline{P} \quad \bar{P}],\\ Q\in[\underline{Q} \quad \bar{Q}]}} a_i], \quad i=0,1,2, [\underline{b}_1 \quad \bar{b}_1]=[\min_{\substack{P\in[\underline{P} \quad \bar{P}],\\ Q\in[\underline{Q} \quad \bar{Q}]}} b_1 \quad \max_{\substack{P\in[\underline{P} \quad \bar{P}],\\ Q\in[\underline{Q} \quad \bar{Q}]}} b_1],$$

It is worth mentioning that these coefficients are dependent, continuous and positive for all admissible values of P and Q. The family of plants can be considered as a subset of the interval plant (4) and hence if the plant (4) is robustly stable, the original family of plants is robustly stable as well, but the converse is not necessarily true. Robust stability of interval plants is often addressed using Kharitonov's theorem [23–27].

3. Mathematical preliminaries

This section briefly reviews some basic results form the area of parametric robust control. For a full comprehensive survey, the reader is referred to Ref. [27].

Definition 1. Consider the set f of all real polynomials of degree n of the from

$$p(s)=a_0+a_1 s+a_2 s^2+\ldots+a_n s^n \tag{5}$$

Where the coefficients vary over independent intervals as follows:

$$a_0=[\underline{a}_0 \quad \bar{a}_0], a_1=[\underline{a}_1 \quad \bar{a}_1], a_2=[\underline{a}_2 \quad \bar{a}_2], \ldots, a_n=[\underline{a}_n \quad \bar{a}_n] \tag{6}$$

Such a set of polynomials is called an interval polynomial. In 1978, Kharitonov presented his celebrated theorem that provides necessary and sufficient conditions for Hurwitz stability of such an interval polynomial.

Theorem 1 ([27]). Every polynomial in the interval family f is Hurwitz-stable if and only if the following Kharitonov polynomials are Hurwitz:

$$\begin{aligned} K^1(s)&=\underline{a}_0+\underline{a}_1 s+\bar{a}_2 s^2+\bar{a}_3 s^3+\underline{a}_4 s^4+\underline{a}_5 s^5+\bar{a}_6 s^6+\ldots \\ K^2(s)&=\underline{a}_0+\bar{a}_1 s+\bar{a}_2 s^2+\underline{a}_3 s^3+\underline{a}_4 s^4+\bar{a}_5 s^5+\bar{a}_6 s^6+\ldots \\ K^3(s)&=\bar{a}_0+\underline{a}_1 s+\underline{a}_2 s^2+\bar{a}_3 s^3+\bar{a}_4 s^4+\underline{a}_5 s^5+\underline{a}_6 s^6+\ldots \\ K^4(s)&=\bar{a}_0+\bar{a}_1 s+\underline{a}_2 s^2+\underline{a}_3 s^3+\bar{a}_4 s^4+\bar{a}_5 s^5+\underline{a}_6 s^6+\ldots \end{aligned} \tag{7}$$

Proof. see [27].

The following notation is necessary before proceeding to the generalization of Kharitonov theorem. Let m be an arbitrary integer and let $\bar{P}(s)=[P_1(s), \quad P_2(s), \quad \ldots, \quad P_m(s)]$ be an *m-tuple* of real interval polynomials where each polynomial $P_i(s)$, $i=1, \ldots, m$ is an interval one. Each polynomial has its four polynomials $K^1(s)$, $K^2(s)$, $K^3(s)$ and $K^4(s)$. If K_m denotes the set of *m-tuples* obtained as follows: for every fixed integer i between 1 and m set $P_i(s)=K_i^k(s)$, $k=1, 2, 3, 4$. Clearly, there are at most 4^m distinct elements in K_m. Further, a family of *m-tuples* called generalized Kharitonov segments are defined as follows:

for any fixed integer l between 1 and m, set $P_i(s) = K_i^k(s)$, $i \neq l$ while for l, suppose that $P_l(s)$ varies in one of the four segments given by $[\,K_l^1(s) \quad K_l^2(s)\,]$, $[\,K_l^1(s) \quad K_l^3(s)\,]$, $[\,K_l^2(s) \quad K_l^4(s)\,]$ and $[\,K_l^3(s) \quad K_l^4(s)\,]$. A segment means all convex combination of two associated vertex polynomials, e.g., a segment $[\,K_l^1(s) \quad K_l^2(s)\,]$ means all convex combinations of the form $(1-\lambda)K_l^1(s) + \lambda K_l^2(s)$, $\lambda \in [\,0 \quad 1\,]$. There are at most $m4^m$ distinct generalized Kharitonov segments, which could be denoted by S_m. The following theorem presents the generalization of Kharitonov theorem.

Theorem 2 ([27]).

I. Given an *m-tuple* of fixed real polynomials $[\,F_1(s), \; F_2(s), \; \ldots, \; F_m(s)\,]$, the polynomial family $P_1(s)F_1(s) + P_2(s)F_2(s) + \ldots + P_m(s)F_m(s)$ is Hurwitz-stable if and only if all the one-parameter polynomial families that result from replacing $[\,P_1(s), \; P_2(s), \; \ldots, \; P_m(s)\,]$ in the above expression by the elements of S_m are all Hurwitz-stable.

II. If the polynomials $F_i(s)$, $i = 1, 2, \ldots, m$ are real and having the form $F_i(s) = s^{t_i}(a_i s + b_i)U_i(s)Q_i(s)$, $i = 1, 2, \ldots, m$, where $t_i \geq 0$ is an arbitrary integer, a_i and b_i are arbitrary real numbers, $U_i(s)$ is an *anti-Hurwitz* polynomial and $Q_i(s)$ is an even/odd polynomial, then it is sufficient that the polynomial families $P_1(s)F_1(s) + P_2(s)F_2(s) + \ldots + P_m(s)F_m(s)$ is *Hurwitz-stable* with the P_i, $i = 1, \ldots, m$ are replaced by the elements of K_m.

Proof. see [27].

4. Parameterization of robust PID-based PSSs

Now consider an interval plant transfer function given by $\mathcal{G}(s) = N_i(s)/D_j(s)$, $i, j = 1, 2, 3, 4$ and a PID controller given by $C(s) = (k_d s^2 + k_p s + k_i)/s$, thus the family of closed loop characteristic polynomials is given by $\Delta(s, k_p, k_i, k_d) = sD(s) + (k_d s^2 + k_p s + k_i)N(s)$. Characterization of the robust PID controllers for an interval plant means to determine the values of k_p, k_i and k_d for which the entire family of the closed loop characteristic polynomials is Hurwitz. Obviously, stabilizing an interval plant by a PID controller does not match the polynomial structure requirements given in Part-II of Theorem 2. Therefore, it is mandatory for synthesizing such a controller to apply the conditions of Part I of the same theorem. Let $NS_i(s)$, $i = 1, 2, 3, 4$ be the four Kharitonov segments associated to $N_i(s)$, $i = 1, 2, 3, 4$ and given by

$$\begin{aligned} &NS_1(s,\lambda) = (1-\lambda)N_1(s) + \lambda N_2(s), \quad NS_2(s,\lambda) = (1-\lambda)N_1(s) + \lambda N_3(s), \\ &NS_3(s,\lambda) = (1-\lambda)N_2(s) + \lambda N_4(s), \quad NS_4(s,\lambda) = (1-\lambda)N_3(s) + \lambda N_4(s), \end{aligned} \tag{8}$$

where $\lambda \in [\,0 \quad 1\,]$. Let $\mathcal{G}_S(s)$ denotes the family of the 16 segment plants given by

$$\mathcal{G}_S(s) = \{G_{ij}(s,\lambda) | G_{ij}(s,\lambda) = \frac{NS_i(s,\lambda)}{D_j(s)}, \quad i, j = 1, 2, 3, 4, \quad \lambda \in [\,0 \quad 1\,]\} \tag{9}$$

The family of closed loop characteristic polynomials for each segment plant $G_{ij}(s, \lambda)$ is denoted by $\Delta_{ij}(s, k_p, k_i, k_d, \lambda)$ and is given by:

$$\Delta_{ij}(s, k_p, k_i, k_d, \lambda) = sD_j(s) + (k_i + k_p s + k_d s^2)NS_i(s, \lambda) \tag{10}$$

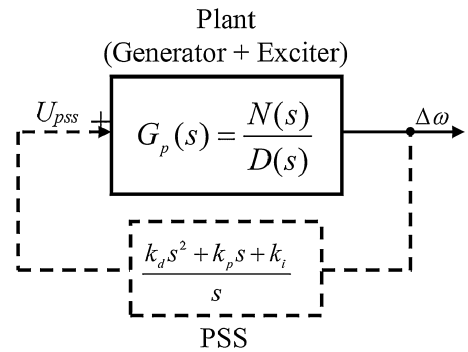

Fig. 2. Positive feedback control system with PID controller.

Therefore, an interval plant $\mathcal{G}(s)$ is stabilized by a particular PID controller if and only if each segment plant $\mathcal{G}_{ij}(s, \lambda) \in \mathcal{G}_S(s)$ is stabilized by that same PID controller. Rather than using these 16 Kharitonov segments, the term $F_2(s) = k_i + k_p s + k_d s^2$ can be decomposed into two properly basis polynomials to suit the polynomial structure in Part II of Theorem 2, as follows $F_2^a(s) = k_i + sk_p$ and $F_2^b(s) = s^2 k_d$. Thus, the synthesis problem is reduced to a stabilization of three interval polynomials as follows:

$$\begin{aligned} \Delta(s, k_p, k_i, k_d) &= F_1(s)D_i(s) + F_2^a(s)N_j(s) + F_2^b(s)N_l(s) \\ &= sD(s) + (k_p s + k_i)N(s) + s^2 k_d N(s), \quad i, j, l = 1, 2, 3, 4 \end{aligned} \tag{11}$$

While sweeping over $\lambda \in [\,0 \quad 1\,]$ is eliminated, such approach results in sixty-four vertex plants and hence increases the computational effort.

4.1. Necessary and sufficient conditions for Hurwitz stability

The positive feedback control system, shown in Fig. 2, has the following closed loop characteristic polynomial:

$$1 - C(s)G_p(s) = 0 \tag{12}$$

Considering the numerator negativity in (1), (10) can be rewritten as follows:

$$sD(s) + (k_d s^2 + k_p s + k_i)N(s) = 0 \tag{13}$$

Since $N(s)$ of (3) is always given by a zero at origin, pole-zero cancelation at origin occurs with the controller pole, and thus (11) can be rewritten as follows:

$$D(s) + (k_d s^2 + k_p s + k_i)N^F(s) = 0 \tag{14}$$

where $N^F(s) = b_1$ for (3) and $N^F(s) = [\,\underline{b}_1 \quad \bar{b}_1\,]$ for (4). The characteristic polynomial of the closed loop system is generally given by:

$$a_0 + b_1 k_i + (a_1 + b_1 k_p)s + (a_2 + b_1 k_d)s^2 + a_3 s^3 + a_4 s^4 = 0 \tag{15}$$

Hurwitz stability of this polynomial is examined using Routh-Hurwitz (RH) criterion. Once more, the coefficients of (3) are positive over the entire range of operating conditions, i.e. $a_i, b_1 > 0$, $i = 0, 1, \ldots, 4$. Typical RH array is constructed as follows:

$$\begin{array}{c|lll} s^4 & a_4 & a_2 + b_1 k_d & a_0 + b_1 k_i \\ s^3 & a_3 & a_1 + b_1 k_p & \\ s^2 & R_{21} = a_3 a_2 + a_3 b_1 k_d - a_1 a_4 - a_4 b_1 k_p & a_3(a_0 + b_1 k_i) & \\ s^1 & R_{11} = (a_3 a_2 + a_3 b_1 k_d - a_1 a_4 - a_4 b_1 k_p)(a_1 + b_1 k_p) - a_3^2(a_0 + b_1 k_i) & & \\ s^0 & R_{01} = a_3(a_0 + b_1 k_i) & & \end{array}$$

Hurwitz stability is guaranteed if and only if the positivity of the first column is ensured, i.e. $R_{i1} > 0$, $i = 0, 1, 2$. It is clear that the positivity of R_{11} infers that of R_{21} for nonnegative k_p. Consequently, stability constraints are reduced to only $R_{01}, R_{11} > 0$. Furthermore, the stability boundaries are given as follows:

$$k_i^{\mathrm{cr}} = \frac{-a_0}{b_1} \tag{16}$$

$$k_d^{\mathrm{cr}} = \left(\frac{a_4 b_1}{a_3 b_1}\right) k_p + \frac{a_1 a_4 - a_2 a_3}{a_3 b_1} + \frac{(a_3/b_1)(a_0 + b_1 k_i)}{a_1 + b_1 k_p} \tag{17}$$

4.2. Kharitonov segment plants

The numerator $N^F(s)$ has only one segment that is given by $NS_1^F(s) = (1-\lambda)\underline{b}_1 + \lambda\bar{b}_1$. Therefore, the PID stabilizer has to stabilize the following segment plants simultaneously:

$$D_i(s) + (k_d s^2 + k_p s + k_i)[(1-\lambda)\underline{b}_1 + \lambda\bar{b}_1] = 0, \quad i = 1, 2, 3, 4 \tag{18}$$

Putting $(1-\lambda)\underline{b}_1 + \lambda\bar{b}_1 = \tilde{b}_1$, the characteristic polynomials of these four segment plants are given as follows:

$$\begin{aligned}
&\underline{a}_0 + \tilde{b}_1 k_i + (\underline{a}_1 + \tilde{b}_1 k_p)s + (\bar{a}_2 + \tilde{b}_1 k_d)s^2 + \bar{a}_3 s^3 + \underline{a}_4 s^4 = 0\\
&\underline{a}_0 + \tilde{b}_1 k_i + (\bar{a}_1 + \tilde{b}_1 k_p)s + (\bar{a}_2 + \tilde{b}_1 k_d)s^2 + \underline{a}_3 s^3 + \underline{a}_4 s^4 = 0\\
&\bar{a}_0 + \tilde{b}_1 k_i + (\underline{a}_1 + \tilde{b}_1 k_p)s + (\underline{a}_2 + \tilde{b}_1 k_d)s^2 + \bar{a}_3 s^3 + \bar{a}_4 s^4 = 0\\
&\bar{a}_0 + \tilde{b}_1 k_i + (\bar{a}_1 + \tilde{b}_1 k_p)s + (\underline{a}_2 + \tilde{b}_1 k_d)s^2 + \underline{a}_3 s^3 + \bar{a}_4 s^4 = 0
\end{aligned} \tag{19}$$

The stability boundaries given by (16) and (17) have to be applied for each segment polynomial in (19). Applying (16) to these segment plants, the minimum critical value of the integral constant can be directly computed as follows:

$$k_i^{\mathrm{cr}} = \min_{\substack{\lambda \in [\,0 \quad 1\,],\\ a_0 \in [\,\underline{a}_0 \quad \bar{a}_0\,]}} \frac{a_0}{\tilde{b}_1} = \frac{-a_0}{\bar{b}_1} \tag{20}$$

By applying (17) to the characteristic polynomials of segment plants at fixed values of $k_p = k_p^*$ and $k_i = k_i^* > k_i^{\mathrm{cr}}$, the minimum critical value of the derivative constant can be directly computed as follows:

$$k_d^{\mathrm{cr}} = \max_{\substack{\lambda \in [\,0 \quad 1\,],\\ k_p = k_p',\\ k_i = k_i' > k_i''}} \begin{bmatrix}
\frac{\underline{a}_4}{\bar{a}_3} k_p^* + \frac{(\underline{a}_1 \underline{a}_4 - \bar{a}_2 \bar{a}_3)}{(\bar{a}_3 \tilde{b}_1)} + \frac{(\bar{a}_3/\tilde{b}_1)(\underline{a}_0 + \tilde{b}_1 k_i^*)}{(\underline{a}_1 + \tilde{b}_1 k_p^*)}\\
\frac{\underline{a}_4}{\underline{a}_3} k_p^* + \frac{(\bar{a}_1 \underline{a}_4 - \bar{a}_2 \underline{a}_3)}{(\underline{a}_3 \tilde{b}_1)} + \frac{(\underline{a}_3/\tilde{b}_1)(\underline{a}_0 + \tilde{b}_1 k_i^*)}{(\bar{a}_1 + \tilde{b}_1 k_p^*)}\\
\frac{\bar{a}_4}{\bar{a}_3} k_p^* + \frac{(\underline{a}_1 \bar{a}_4 - \underline{a}_2 \bar{a}_3)}{(\bar{a}_3 \tilde{b}_1)} + \frac{(\bar{a}_3/\tilde{b}_1)(\bar{a}_0 + \tilde{b}_1 k_i^*)}{(\underline{a}_1 + \tilde{b}_1 k_p^*)}\\
\frac{\bar{a}_4}{\underline{a}_3} k_p^* + \frac{(\bar{a}_1 \bar{a}_4 - \underline{a}_2 \underline{a}_3)}{(\underline{a}_3 \tilde{b}_1)} + \frac{(\underline{a}_3/\tilde{b}_1)(\bar{a}_0 + \tilde{b}_1 k_i^*)}{(\bar{a}_1 + \tilde{b}_1 k_p^*)}
\end{bmatrix} \tag{21}$$

In Eq. (21), "max" refers to the maximum element in the vector while λ varies over $[\,0 \quad 1\,]$ with fixed values of k_p and k_i. Assuming fixed value of k_i, the critical values of k_d can be computed for a range of k_p by sweeping over $\lambda \in [\,0 \quad 1\,]$ at each value of k_p. This numerical algorithm has to be repeated with different values of k_i to scan the three-dimensional space of the controller parameters.

4.3. Kharitonov vertex plants

This approach can avoid sweeping over $\lambda \in [\,0 \quad 1\,]$ by considering additional vertex plants. These additional plants come out from the decomposition of the controller into two parts, i.e. $C^a(s) = k_i + sk_p$ and $C^b(s) = s^2 k_d$. Such vertex systems have the following characteristic polynomials:

$$D_i(s) + C^a(s)N_j^c(s) + C^b(s)N_l^c(s) = 0, \quad i = 1, 2, 3, 4 \quad j, l = 1, 2 \tag{22}$$

Eq. (22) describes sixteen characteristic polynomials for example if $i = 1$ and $j, l = 1, 2$

$$\begin{aligned}
&\underline{a}_0 + \underline{b}_1 k_i + (\underline{a}_1 + \underline{b}_1 k_p)s + (\bar{a}_2 + \underline{c}_1 k_d)s^2 + \bar{a}_3 s^3 + \underline{a}_4 s^4 = 0\\
&\underline{a}_0 + \underline{b}_1 k_i + (\underline{a}_1 + \underline{b}_1 k_p)s + (\bar{a}_2 + \bar{c}_1 k_d)s^2 + \bar{a}_3 s^3 + \underline{a}_4 s^4 = 0\\
&\underline{a}_0 + \bar{b}_1 k_i + (\underline{a}_1 + \bar{b}_1 k_p)s + (\bar{a}_2 + \underline{c}_1 k_d)s^2 + \bar{a}_3 s^3 + \underline{a}_4 s^4 = 0\\
&\underline{a}_0 + \bar{b}_1 k_i + (\underline{a}_1 + \bar{b}_1 k_p)s + (\bar{a}_2 + \bar{c}_1 k_d)s^2 + \bar{a}_3 s^3 + \underline{a}_4 s^4 = 0
\end{aligned} \tag{23}$$

where $\underline{c}_1 = \underline{b}_1$, $\bar{c}_1 = \bar{b}_1$. The letter c is considered to distinguish the multiplier of k_d form that of k_p and k_i. Necessary and sufficient stability constraints (16) and (17) obtained for the general polynomial (15) are applied to the sixteen vertex polynomials. While applying the constraint (17), the term $(a_4 b_1/a_3 b_1)k_p$ has to be replaced by $(a_4 b_1/a_3 c_1)k_p$ to account for difference in the coefficients between k_p and k_d imposed by decomposition and therefore such constraint (18) has to be rewritten as follows:

$$k_d^{\mathrm{cr}} = \frac{a_4 b_1}{a_3 c_1} k_p + \frac{a_1 a_4 - a_2 a_3}{a_3 c_1} + \frac{(a_3/c_1)(a_0 + b_1 k_i)}{(a_1 + b_1 k_p)} \tag{24}$$

The constraint (16) is satisfied for the sixteen polynomial if and only if $k_i > -\underline{a}_0/\bar{b}_1$, which agrees with (20). The critical value of the derivative gain is computed for the 16 polynomials by (17) for fixed k_p and k_i where the critical k_d is computed as follows:

$$k_d^{\mathrm{cr}} = \max_{\substack{k_p = k_p^*,\\ k_i = k_i^*}} \begin{bmatrix}
\frac{\underline{a}_4 \underline{b}_1}{\bar{a}_3 \underline{c}_1} k_p + \frac{\underline{a}_1 \underline{a}_4 - \bar{a}_2 \bar{a}_3}{\bar{a}_3 \underline{c}_1} + \frac{(\bar{a}_3/\underline{c}_1)(\underline{a}_0 + \underline{b}_1 k_i)}{\underline{a}_1 + \underline{b}_1 k_p}\\
\frac{\underline{a}_4 \underline{b}_1}{\bar{a}_3 \bar{c}_1} k_p + \frac{\underline{a}_1 \underline{a}_4 - \bar{a}_2 \bar{a}_3}{\bar{a}_3 \bar{c}_1} + \frac{(\bar{a}_3/\bar{c}_1)(\underline{a}_0 + \underline{b}_1 k_i)}{\underline{a}_1 + \underline{b}_1 k_p}\\
\vdots\\
\frac{\bar{a}_4 \bar{b}_1}{\underline{a}_3 \bar{c}_1} k_p + \frac{\bar{a}_1 \bar{a}_4 - \underline{a}_2 \underline{a}_3}{\underline{a}_3 \bar{c}_1} + \frac{(\underline{a}_3/\bar{c}_1)(\bar{a}_0 + \bar{b}_1 k_i)}{\bar{a}_1 + \bar{b}_1 k_p}
\end{bmatrix} \begin{matrix} \Delta_{111}\\ \Delta_{112}\\ \vdots\\ \Delta_{422} \end{matrix} \tag{25}$$

In (25), "max" refers to the maximum entry of this vector at fixed values of k_p and k_i. A marginal stability surface is developed in the space of the controller parameters by considering a fine grid in $k_p \times k_i$.

5. Parameterization of robust phase-lead PSSs

According to Theorem 2, the design of robust phase-lead compensators is carried out for Kharitonov vertex plants only. The design algorithm aims to compute the robust stabilizing compensators. The closed loop system using the proposed phase-lead stabilizer is shown in Fig. 3. Consider a phase-lead stabilizer having a transfer function given by:

$$C(s, K, T_1, T_2) = \frac{K(1 + T_1 s)}{1 + T_2 s} \tag{26}$$

The positive feedback control system shown in Fig. 3, has the following closed loop characteristic polynomial:

$$(1 + T_2 s)D(s) + K(1 + T_1 s)N(s) = 0 \tag{27}$$

Consider the plant (3) and the controller (26), (27) can be rewritten as follows:

$$\begin{aligned}
&T_2 a_4 s^5 + (T_2 a_3 + a_4)s^4 + (T_2 a_2 + a_3)s^3\\
&\quad + (T_2 a_1 + a_2 + KT_1 b_1)s^2 + (T_2 a_0 + a_1 + Kb_1)s + a_0 = 0
\end{aligned} \tag{28}$$

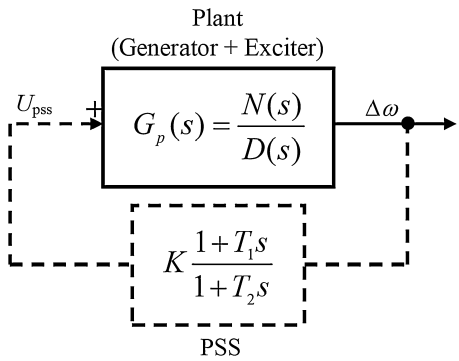

Fig. 3. Positive feedback control system with phase-lead compensator.

Typical RH array for (28) is constructed as follows:

s^5	T_2a_4	$T_2a_2+a_3$	$T_2a_0+a_1+Kb_1$
s^4	$T_2a_3+a_4$	$T_2a_1+a_2+KT_1b_1$	a_0
s^3	$R_{31}=(T_2a_3+a_4)(T_2a_2+a_3)-T_2a_4(T_2a_1+a_2+KT_1b_1)$	$(T_2a_3+a_4)(T_2a_0+a_1+Kb_1)-T_2a_4a_0$	
s^2	$R_{21}=R_{31}(T_2a_1+a_2+KT_1b_1)-R_{32}(T_2a_3+a_4),$	a_0R_{31}	
s^1	$R_{11}=R_{21}R_{32}-R_{22}R_{31}$		
s^0	$R_{01}=a_0R_{31}$		

Stability of polynomial (28) is enforced if and only if $R_{i1}>0$, $i=1, 2, 3$. Unlike PID controller, no explicit formulas are deduced for phase lead compensator. A typical range of a PSS pole time-constant in industry is frequently given by $T_2=[\,0.02 \quad 0.15\,]$ s, i.e. PSS design is typically carried out with some value in this interval [2]. Hence, robust stability boundaries for a given $T_2=T_2^*$ are expressed as follows:

$$R_{i1}(K,T_1)\big|_{T_2=T_2^*}=0, \quad i=1,2,3 \tag{29}$$

These boundaries can be generalized by $f(x,y)=0$ and be plotted using MATLAB function "*ezplot*". Necessary and sufficient condition for the existence of the solution set, that contains the stabilizing phase lead stabilizers, can be stated as:

$$\bigcap_{T_2=T_2^*,\quad i=1,2,3} R_{i1}(K,T_1)\neq\varnothing \tag{30}$$

To guarantee robust stability, such controller has to stabilize the eight vertex plants of the interval plant model (4) simultaneously, i.e. the following eight characteristic polynomials are Hurwitz.

$$(1+T_2s)D_i(s)+K(1+T_1s)N_j(s)=0, \quad i=1,2,3,4, \quad j=1,2 \tag{31}$$

Considering the eight vertex plants, sufficient constraint for the existence of the solution set that contains the robust stabilizing phase lead stabilizers can be rewritten as follows:

$$\bigcap_{i=1,2,3,4,\quad j=1,2,\quad k=1,2,3} R_{k1}^{ij}(K,T_1)\Big|_{T_2=T_2^*}\neq\varnothing \tag{32}$$

6. Simulation results

The main result of this paper focuses on the computation of the admissible parameters of the three-term PSSs that guarantee robust stability under wide range of operating points. Results based on the interval plant model (4) are presented for both PID controller and phase-lead compensator. It is assumed that active and reactive powers at the generator bus vary over the following intervals:

$$P\in[\,0.2 \quad 1\,], \quad Q\in[\,-0.2 \quad 0.5\,] \tag{33}$$

Typically, these intervals encompass all practical operating points [10,11]. Further, any point that belongs to these ranges has a steady load flow solution. The coefficients of (3) are calculated for 1024 mesh points that belong to $[\,0.2 \quad 1\,]\times[\,-0.2 \quad 0.5\,]$ where their bounds are computed and given by:

$$a_4=[\,1 \quad 1\,],\ a_3=[\,20.46 \quad 20.46\,],\ a_2=[\,22.41 \quad 87.21\,],$$
$$a_1=[\,131.5 \quad 793\,],\ a_0=[\,570 \quad 1763.7\,],\ b_1=[\,2.44 \quad 11.57\,] \tag{34}$$

6.1. Robust stabilization via PID-based PSSs

The design is carried out based on the interval plant model (4) while the bounds of its coefficients are given by (34). The results are presented for the case of nonnegative proportional gains and an arbitrary interval is taken as $k_p=[\,0 \quad 500\,]$. Negative proportional gains present supplementary phase-lag and hence it is not considered. However, a PID controller may exist for such a negative gain.

6.1.1. Segment plants

If we consider the negative values of the integral gain, the minimal allowable value of k_i is given by (20) which results in $k_i^{cr}=-49.24$ and hence if $k_i=[\,-49.24 \quad 200\,]$; the critical values of k_d can be calculated explicitly as given in (21). The upper bound of k_i is randomly chosen. The marginal stability surface in the controller parameter space is shown in Fig. 4. To simplify the illustration, the critical values of the derivative gain are plotted against the proportional gains at constant values of the integral gain as shown in Fig. 5.

6.1.2. Vertex plants

The minimal critical value of the integral gain is not altered between segment and vertex plants and given by $k_i^{cr}=-49.24$. The unconstrained maximization (25) computes the critical value of the derivative gain for a pre-specified pair (k_p^*, k_i^*) considering the intervals (33). The critical surface is computed for the ranges of k_p and k_i as shown in Fig. 6. For clear illustration, the critical values of k_d for the range of k_p is shown in Fig. 7 for fixed values of k_i.

6.2. Robust stabilization via phase-lead PSSs

Characterization of the robust phase-lead PSSs is accomplished based on interval plant model (4). Firstly, the computation of the stabilizing PSSs for a nominal plant is considered for $P=1.0$ and $Q=-0.2$. The time constant of the stabilizer pole is selected at 0.05 s. After computing the coefficients, Matlab function "*ezplot*" is utilized to plot the constraints (29). Fig. 8 shows the plot of the three constraints and it is noticed that they all tolerate with $R_{11}=0$, i.e. the stability region is that bounded by R_{11} only. The effect of the pole time constant on the stability region is considered where stability regions for different values are shown in Fig. 9. Remarkably, small values of the pole time constant have the effect of extended stability regions.

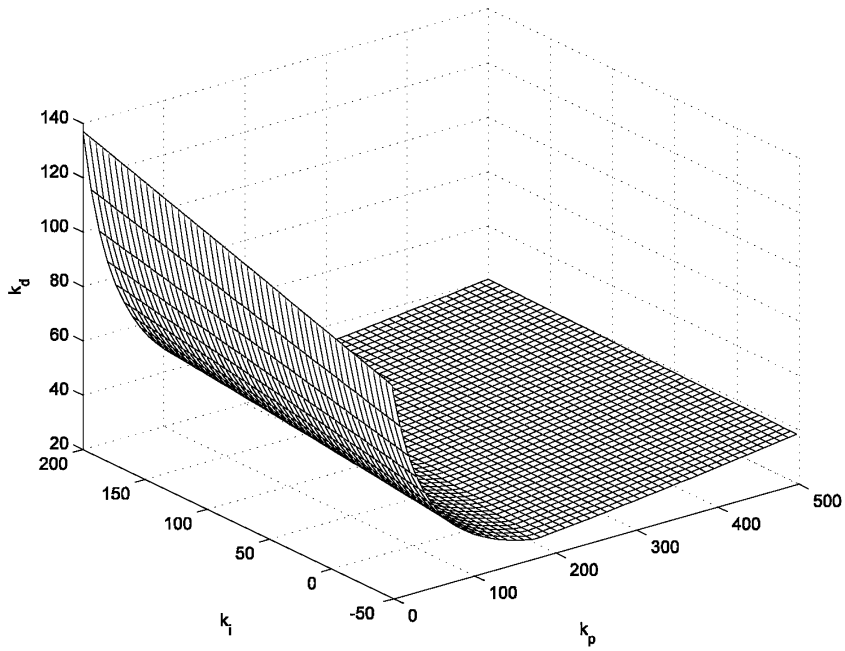

Fig. 4. PID parameters space developed using segment plant.

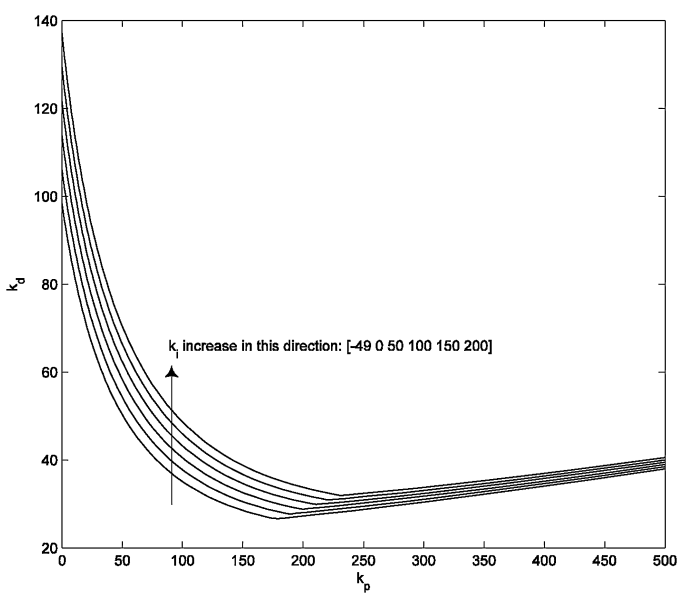

Fig. 5. Robust stability regions on k_p–k_d parameter-plane for fixed values of k_i using segment plants.

Using the coefficients bounds (34), the constraint (32) is not satisfied, i.e. the constraint (29) does not tolerate in a common region for the eight vertex plants with $T_2 = 0.05$ s. To overcome this problem, a smaller pole time constant can be considered, e.g., $T_2 = 0.02$ s, or the ranges (33) have to be narrowed down to $P = [0.4\ 1.0]$ pu, $Q = [-0.1\ 0.5]$ pu at $T_2 = 0.05$ s. The latter suggestion is adopted where the stability region is shown in Fig. 10.

6.3. Applicant controller validation based on linear model

The poles of the uncontrolled plants are firstly computed to illustrate the poor damping characteristics and even instability of some operating points. The damping ratios of the dominant poles of 1024 mesh plants in (33) are shown in Fig. 11, which indicates negative damping for some plants, i.e. unstable plants. An applicant PID stabilizer is selected as $k_p = 100$, $k_i = -20$ and $k_d = 70$ and the closed loop poles are computed where damping ratios of the dominant poles are shown in Fig. 12. Remarkably, a minimum damping ratio, that is greater than 0.3, is achieved for the entire family of plants. Furthermore, a phase-lead PSS is selected as $K = 50$, $T_1 = 0.5$ s and $T_2 = 0.05$ s and the closed loop poles are computed where damping rations of the dominant poles are similarly shown in Fig. 13.

Hint: Although the robust phase-lead stabilizer is designed for a narrow operating range, the controller considered for simulation can stabilize all plants in the full range (33) because the suggested approach presents sufficient but not necessary stability constraints (*conservative results*).

6.4. Applicant controller validation based on nonlinear model

The nonlinear model of the considered system, which is given in Appendix, is stimulated using the controllers' parameter setting selected before. The response of the closed loop system due a 10% step change in mechanical torque is shown in Fig. 14. The proposed PSS designs are both tested at an operating point determined by $P_g = 0.9$ and $Q_g = 0.2$ pu. Remarkably, the proposed robust PSSs can ensure system stability at this test point.

6.5. Multimachine simulation

The proposed design can be applied to multi-machine power systems by designing a PSS for one machine at a time and considering the rest of the system as an infinite bus. The resulting control is decentralized or local as it uses speed deviation only from the generator on which it is installed. Local PSSs have the following advantages: (i) effective in damping local modes, (ii) no communication network is needed to transfer data to a centralized controller, thus cost-effective, and (iii) time delays are avoided. The purpose of this section is to demonstrate the merits of the proposed PSS design methodology based on a more realistic model. The two-area four-machine test power system shown in Fig. 15 and proposed in Ref. [2] is utilized in this study because it is accepted in the literature as a tool to study the inter-area mode of oscillations. Further, this system is available as a MATLAB/SIMULINK demo program [28]. In

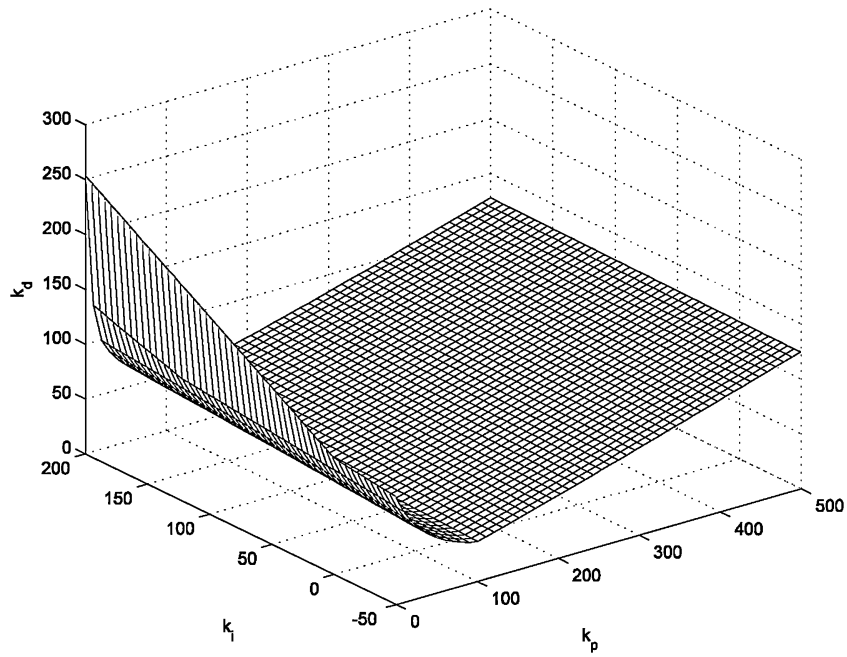

Fig. 6. PID parameters space developed using vertex plants.

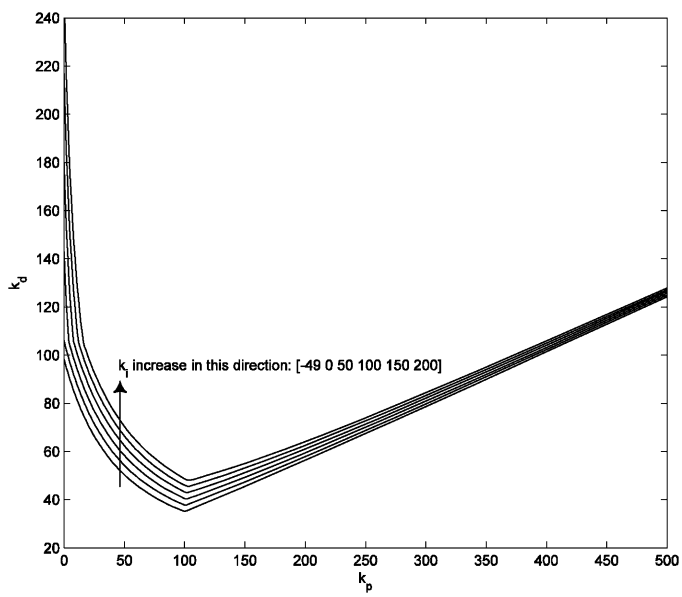

Fig. 7. Robust stability regions on k_p–k_d parameter-plane for fixed values of k_I using vertex plants.

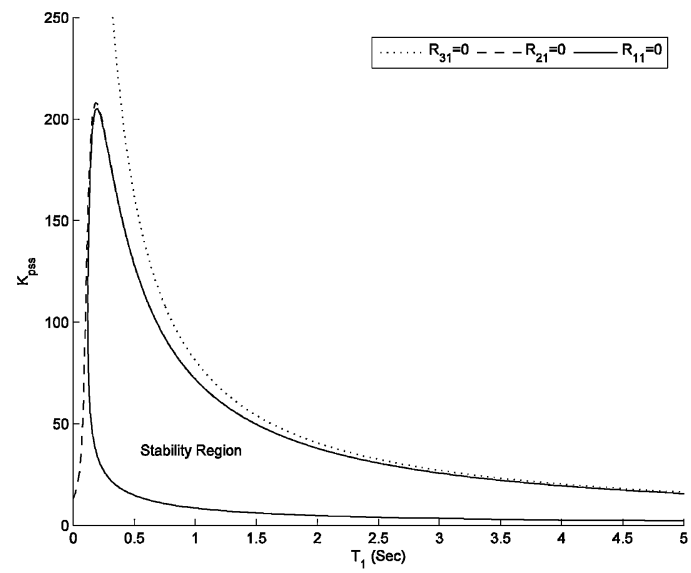

Fig. 8. Plot of stability boundaries $R_{31} = 0$, $R_{21} = 0$, and $R_{11} = 0$ for sample operating point with $T_2 = 0.05$ s.

addition, it is equipped with well-tuned power system stabilizers including the standard IEEE PSS4B [29] and the conventional PSS [2]. This gives credit to the comparison with the proposed PSS.

The test system consists of two fully symmetrical areas linked together by two 230 kV lines of 220 km length. It is specifically designed to study low frequency electromechanical oscillations in large interconnected power systems. Each area is equipped with two identical round rotor generators rated 20 kV/900 MVA. The synchronous machines have identical parameters except for the inertias which are $H = 6.5$ s in area-1 and $H = 6.175$ s in area-2. Thermal plants having identical speed regulators are further assumed at all locations, in addition to fast static exciter with a gain of 200. Saturation limits are imposed on both excitation voltages (E_{fd}) and the supplementary signals (U) as specified in Ref. [2]. The loads are represented by constant impedances and split between the two areas. Therefore, the equivalent single-machine subsystems are roughly identical due system symmetry. Consequently, the design is carried out once for one equivalent subsystem whilst the resulting stabilizer is added to the four machines.

Since damping and frequency of inter-area oscillations depend mainly on the quantity of the tie-line power, different operating points that result in different tie-line powers ranging from 200 MW to 600 MW are considered, which allows for ±50% perturbation around the nominal tie-line power. The values of P and Q at each machine-bus are computed through a load flow study for different operating points where the corresponding ranges are given by:

$$P = [\,0.5 \quad 0.9\,] \,\&\, Q = [\,0.2 \quad 0.5\,].$$

Remark 1. Multimachine power system is a multi-input multi-output (MIMO) system and hence it violates theoretically the

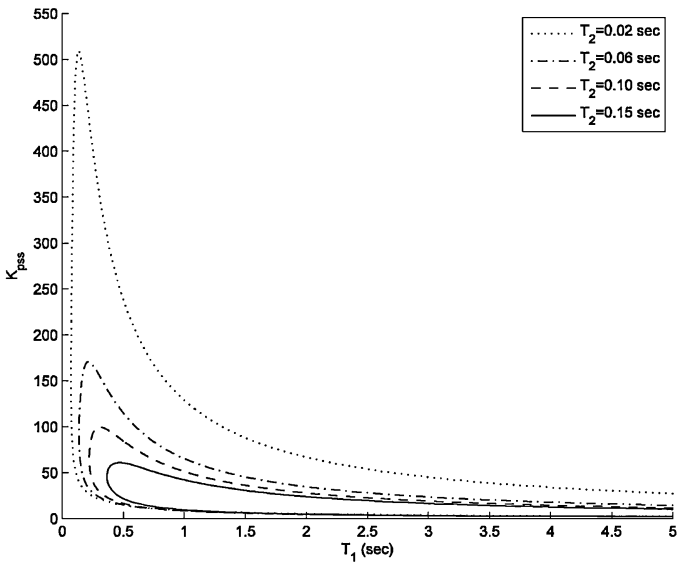

Fig. 9. Stability regions for fixed values of the pole time constant (T_2) for sample test point (P = 1.0 pu, Q = −0.2 pu).

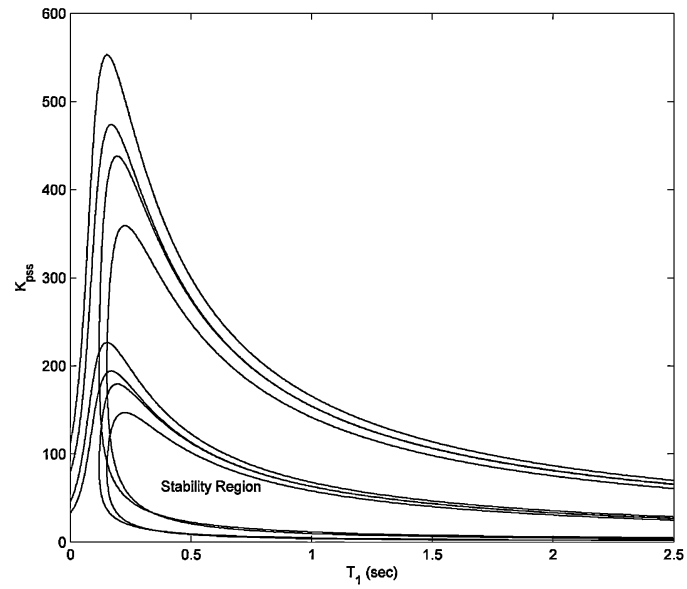

Fig. 10. Stability regions for the eight vertex-plants while P = [0.4 1.0] pu, Q = [−0.1 0.5] pu and T_2 = 0.05 s.

basic requirements of the proposed approach because it is not a SISO system and it has many PSSs that have more than three terms. Consequently, the proposed approach cannot be applied to multimachine systems directly. Firstly, a multimachine system is decomposed into a set of single-machine subsystem using Thevenin theorem. Each subsystem comprises one machine connected to hypothetical infinite bus through an equivalent tie line. This decomposition enables us to consider the uncertainties in P and Q of each machine separately.

Remark 2. The decomposition approach, which is proposed to consider the multimachine case, neglects the interaction between different control loops. No one can claim that the interactions between different control loops have no effect in the control design. However, Baker et al. [30] proved that the interaction between excitation systems becomes significant when the machines are closely tied electrically.

The constraints presented in Sections 4 and 5 are utilized to compute the controller stability regions as before. An applicant PID-based PSS parameters are selected as $k_p = 30$, $k_i = 50$, $k_d = 1$ while an applicant phase-lead based PSS parameters are selected as $k_{pss} = 40$, $T_1 = 0.5$ s, $T_2 = 0.02$ s. The effectiveness of the proposed designs to suppress both local and inter-area modes of oscillations is investigated by small and large-scale disturbances. Firstly, the system response due to 10% increment in the load of Area #2 is shown in Fig. 16. Secondly, the system is tested for a three-phase to ground short circuit and the response is depicted in Fig. 17. Noticeably, the standard IEEE-PSS4B stabilizer [29] and the conventional design

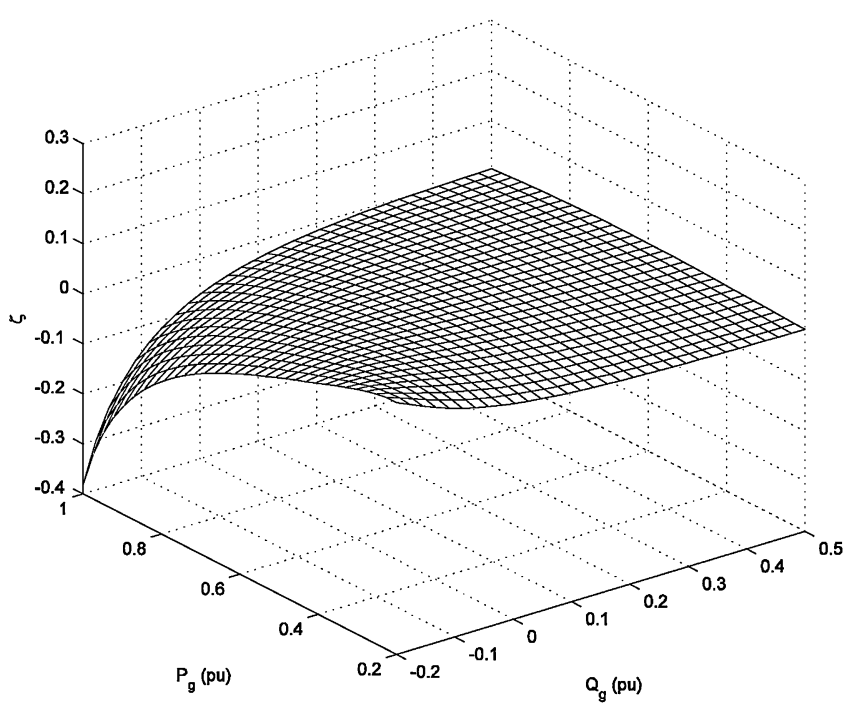

Fig. 11. Damping ratios of the dominant open loop poles of 1024 points in Ref. [33].

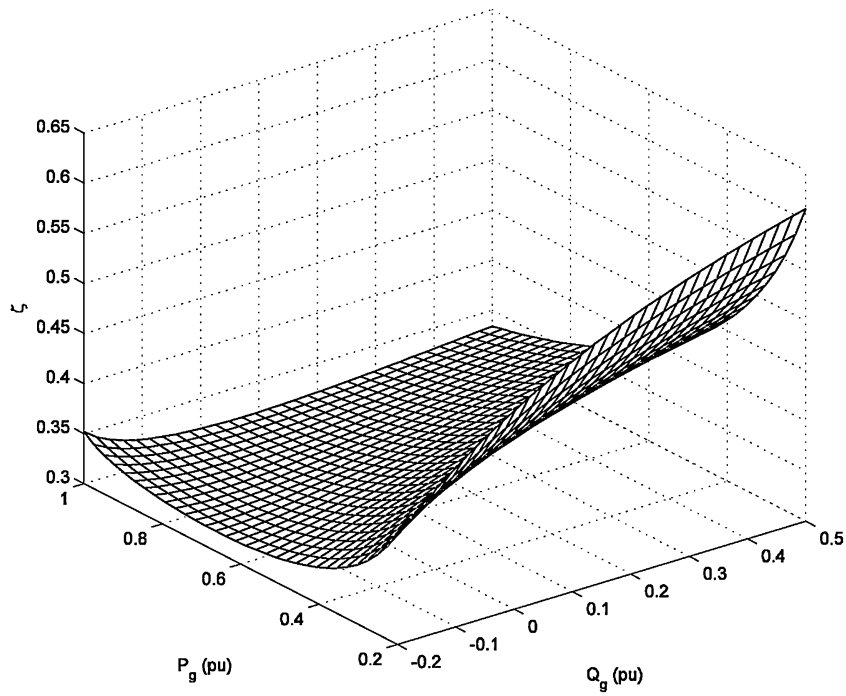

Fig. 12. Damping ratios of the dominant closed loop poles of 1024 points in [33] using PID stabilizer with $k_p = 100$, $k_i = -20$, $k_d = 70$.

presented in Ref. [2] failed to maintain system stability. Moreover, Figs. 16 and 17 present the response of the PID design reported in Ref. [15] for fair comparison with the proposed PID design. The proposed PID-based PSS outperforms the PID-based PSS presented in Ref. [15], as shown in Fig. 16 for small disturbance, in terms of overshooting and settling time. However the latter outperforms the former in case of large disturbance, as shown in Fig. 17. Remarkably, the responses of the proposed controllers, CPSS, and IEEE-PSS4B, shown in Fig. 16, have the same steady state operating point while the PID-based PSS in Ref. [15] has different steady state point. This may be explained by the fact that the interaction between all controllers was considered in Ref. [15] while such interaction is not considered in the proposed design and CPSS design because the design is carried out on the basis of single-machine infinite-bus model.

Remark 3. Multimachine simulations were carried out to confirm the effectiveness of the proposed method in designing PSSs based on the classical approach of single-machine infinite-bus system (SMIB). Consequently, the size of a real system comprising m-machines has no effect on the results because the proposed approach is applied m-times to the m single-machine subsystems. However, the ultimate solution of stabilization of low-frequency oscillations of a multimachine should be a multimode stabilizer

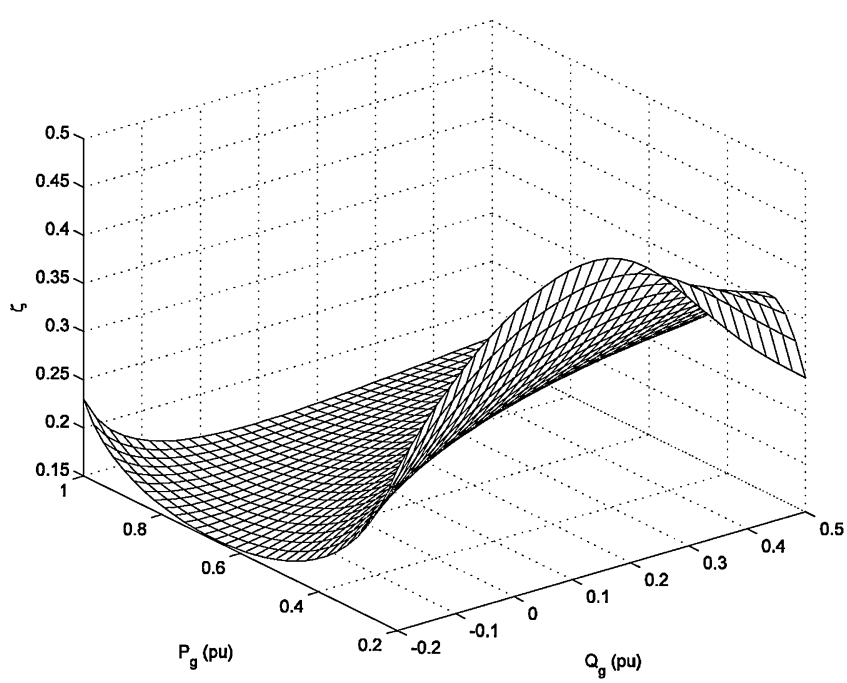

Fig. 13. Damping ratios of the closed loop poles of 1024 points in [33] using phase-lead stabilizer with $k_{pss} = 50$, $T_1 = 0.5$ s, $T_2 = 0.05$ s.

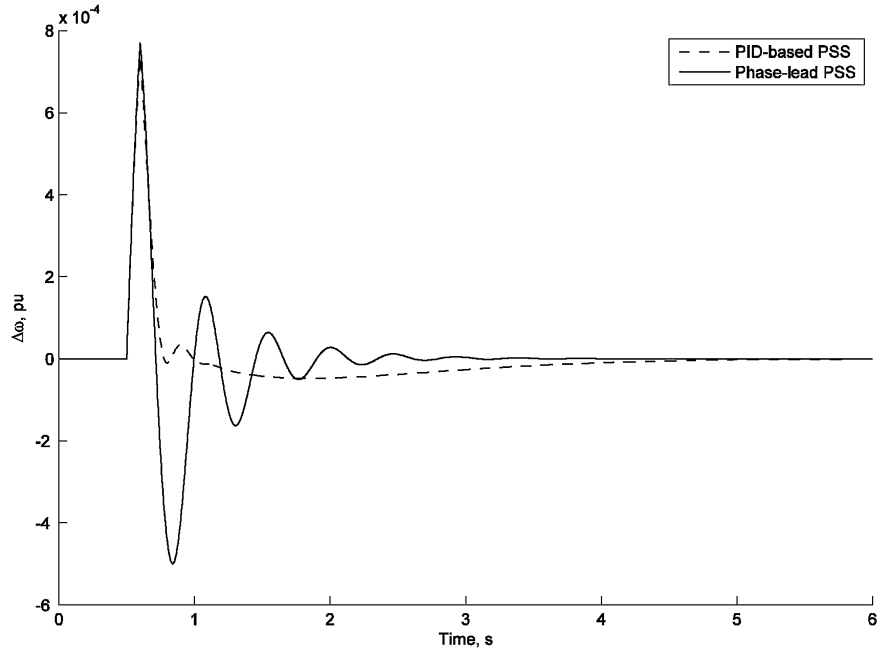

Fig. 14. Speed deviation due to 0.1 pu step increment in mechanical torque for 0.1 s with different controllers.

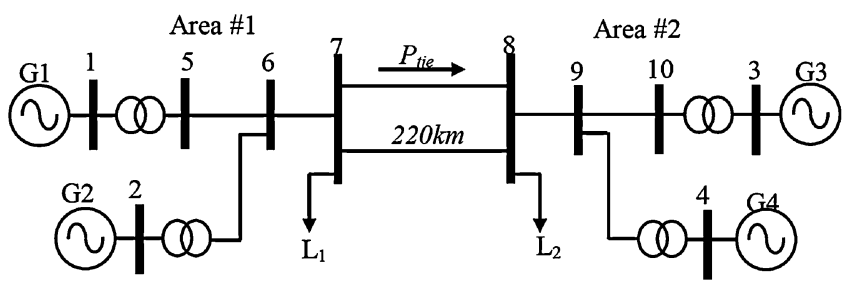

Fig. 15. Two-area four-machine test power system [3].

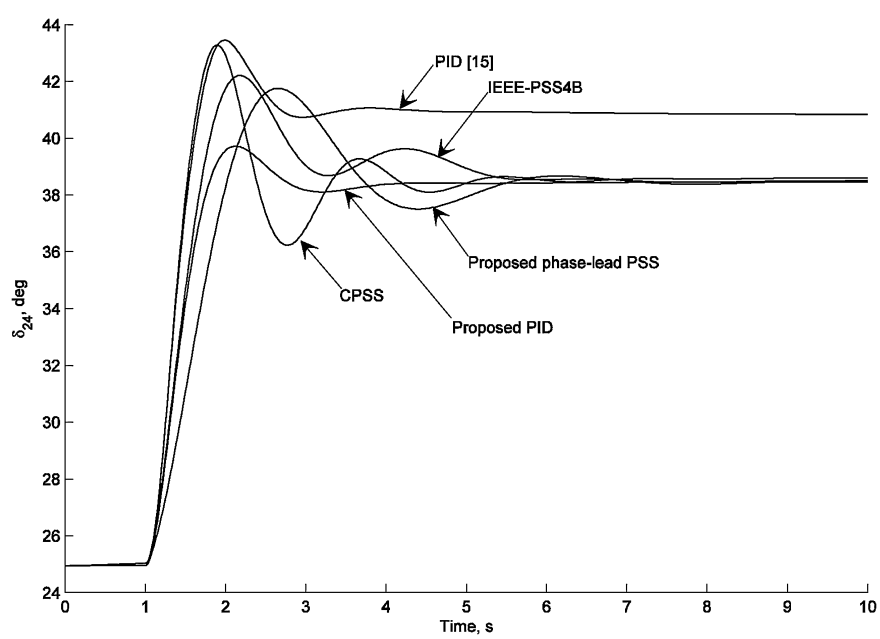

Fig. 16. System response due to 10% increment in the load of Area #2.

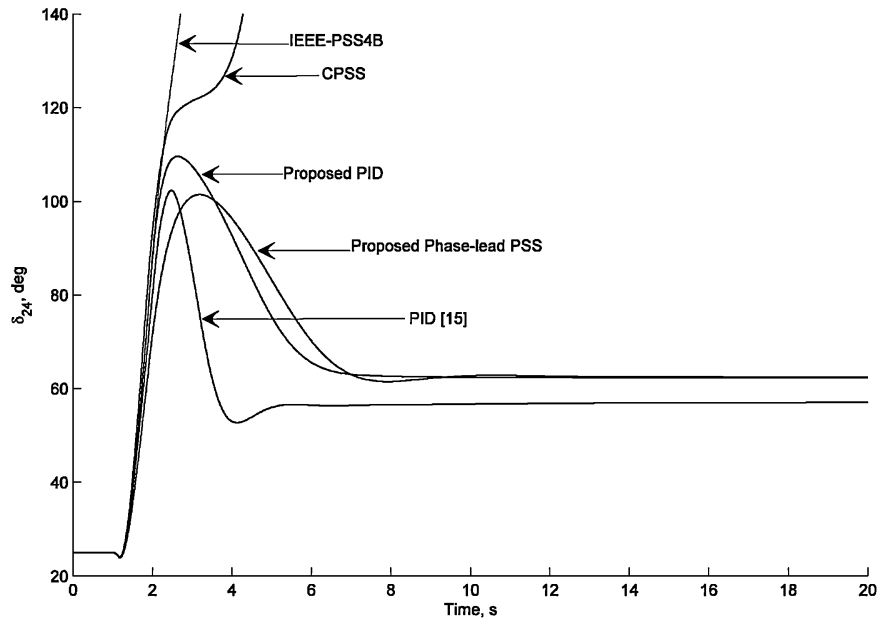

Fig. 17. System response due to three-phase to ground fault on one tie line at 70 km far from Bus #8 for 133 ms.

design based on the multimachine model. However, the results obtained, based on SMIB models, have confirmed the effectiveness of proposed approach to compute a set of decentralized feasible controllers in a multimachine system.

6.6. Discussion and comments

The proposed design approach assumes the textbook version of a PID controller to carry out this study. Therefore, one may comment the problem of sensor noise due to the inclusion of pure derivative term. Such a comment can be by considered in the design approach by using a high pass filter with appropriate corner frequency to implement the derivative action. Corner frequency can be selected to account for the frequency range of the electromechanical modes at different operating points. The proposed technique has been applied to a single-machine infinite-bus system equipped with a three-term controller. These simple models are primarily used to demonstrate the principles of the proposed technique. However, further research is currently under way to extend the application to the design of robust decentralized PSSs in multimachine power system. Kharitonov's theorem presents the necessary and sufficient conditions for Hurwitz stability of an interval polynomial on condition that the coefficients of such polynomial vary over independent intervals. In our case, the coefficients of the interval polynomial (2) are not independent because any variation in P, Q, or both makes all coefficients to vary simultaneously. Consequently, any change in one coefficient implies simultaneous changes in the others. This fact makes the results derived via Kharitonov's theorem "conservative". Therefore, in the controllers' parameter plane point of view, the described stability region is a subset of a larger one.

7. Conclusion

This paper presents a simple analytical method for computing the set of robust three-term stabilizing PSSs. An interval plant is developed to capture uncertainties in the parameters of the power system model imposed by constantly variation in the operating point. Stabilization of the proposed interval plant by PID controller and phase lead compensator based PSSs are dealt with using generalized Kharitonov's theorem. Necessary and sufficient constraints for characterizing the robust stabilizing three-term controllers are derived by applying RH criterion to a set of segment/vertex plants where the region of robust stability comes out from the intersection of the stability regions of all segment/vertex plants. The synthesis of robust PID based PSS is reduced to simultaneous stabilization of either four segment plants or sixteen vertex plants. It is remarked that using segment approach gives more relaxed stability constraints than that obtained from using the vertex approach, i.e. the stability region computed for vertex plants is always smaller than that computed using segment plants. Simulation results of applicant PID and Phase-lead stabilizers confirm the effectiveness of the proposed approach in damping low frequency oscillations that follow both small and large disturbances. The design methodology applies only to a single-machine infinite-bus system equipped with a three-term controller. These simple models have demonstrated the principles of the proposed technique. However, further research is currently under way to extend the application to the design of robust decentralized PSSs in multimachine power system without decomposing it into single-machine subsystems.

Appendix.

A.1. Nonlinear model and data of a single-machine infinite-bus test system:

$$\begin{aligned}
\dot{\delta} &= \omega_o \omega, \\
\dot{\omega} &= \frac{T_m - (E'_q I_q + (X_q - X'_d) I_d I_q)}{M}, \\
\dot{E}'_q &= -\frac{E'_q + (X_d - X'_d) I_d - E_{fd}}{T'_{do}}, \\
\dot{E}_{fd} &= \frac{K_E V_{ref} + U_{pss} - K_E V_T - E_{fd}}{T_E},
\end{aligned} ,$$

$$-(X_e + X_q) I_q + V^\infty \sin\delta = 0$$

$$(X_e + X'_d) I_d + E'_q + V^\infty \cos\delta = 0$$

$$X_d = 1.6 \quad \text{pu}, \quad X_q = 1.55 \quad \text{pu}, \; X'_d = 0.32 \quad \text{pu},$$
$$T'_{do} = 6 \quad \text{s}, \quad M = 10 \quad \text{s}, \quad K_E = 25, \quad T_E = 0.05 \quad \text{s},$$
$$E_{fd}^{min} = -5 \quad \text{pu}, \; E_{fd}^{max} = 5 \quad \text{pu},$$
$$V^{\infty} = 1 \quad \text{pu}, \quad \omega_o = 314.159 \quad \text{rad/s}, \quad \text{Rating} = 100 \quad \text{MVA}$$

A.2. Coefficients of the transfer function of the system shown in Fig. 1 in terms of k_1–k_6 and machine parameters:

$$\tilde{a}_4 = Mk_3T'_{do}T_E, \quad \tilde{a}_3 = M(k_3T'_{do} + T_E), \quad \tilde{a}_2 = M + \omega_o k_1 k_3 T'_{do} T_E + K_E k_3 k_6 M, \quad \tilde{a}_1 = \omega_o k_1 (k_3 T'_{do} + T_E) - \omega_o k_2 k_3 k_4 T_E,$$
$$\tilde{a}_0 = \omega_o(k_1 - k_2k_3k_4 - K_Ek_2k_3k_5 + K_Ek_1k_3k_6), \quad \tilde{b}_1 = K_Ek_2k_3.$$

Since $\tilde{a}_4$ is always fixed (load-independent), both numerator and denominator are divided by $\tilde{a}_4$ to get strictly proper monotonic transfer function whose coefficients are computed at any operating point as follows:

$$a_4 = \frac{\tilde{a}_4}{\tilde{a}_4} = 1, \quad a_3 = \frac{\tilde{a}_3}{\tilde{a}_4}, \quad a_2 = \frac{\tilde{a}_2}{\tilde{a}_4}, \quad a_1 = \frac{\tilde{a}_1}{\tilde{a}_4}, \quad a_0 = \frac{\tilde{a}_0}{\tilde{a}_4}, \quad b_1 = \frac{\tilde{b}_1}{\tilde{a}_4}.$$

References

[1] P.W. Sauer, M.A. Pai, Power System Dynamics and Stability, Prentice-Hall, Inc., New Jersey, 1998.
[2] P. Kundur, Power System Stability and Control, McGraw-Hill, New York, 1994.
[3] F.P. DeMello, C. Concordia, Concepts of synchronous machine stability as affected by excitation control, IEEE Trans. Power Appar. Syst. 88 (April (4)) (1969) 316–329.
[4] E.V. Larsen, D.A. Swann, Applying power system stabilizers: parts I–III, IEEE Trans. Power Appar. Syst. 100 (June (6)) (1981) 3017–3046.
[5] S. Chen, O. Malik, H_∞ optimization-based power system stabilizer design, IEE Proc. Gen. Transm. Distrib. 142 (March (2)) (1995) 179–184.
[6] G.N. Taranto, J.K. Shiau, J.H. Chow, H. Othman, Robust decentralized design of multiple FACTS controllers, IEE Proc. Gen. Transm. Distrib. 144 (1) (1997) 61–67.
[7] M. Djukanovic, M. Khammash, V. Vittal, Application of the structured singular value theory for robust stability and control analysis of multimachine power systems. Parts I, II, IEEE Trans. Power Syst. 13 (4) (1998) 1311–1322.
[8] M. Djukanovic, M. Khammash, V. Vittal, Sensitivity based structured singular value approach to stability robustness of power systems, IEEE Trans. Power Syst. 15 (May (2)) (2000) 825–830.
[9] M. Djukanovic, M. Khammash, V. Vittal, Sequential synthesis of structured singular value based decentralized controllers in power systems, IEEE Trans. Power Syst. 14 (2) (1999) 635–644.
[10] R. Castellanos, A.R. Messina, H. Sarmiento, Robust stability analysis of large power systems using the structured singular value theory, Electr. Power Energy Syst. 27 (2005) 389–397.
[11] R. Castellanos, A.R. Messina, H. Sarmiento, A μ-analysis approach to power system stability robustness evaluation, Electr. Power Syst. Res. 78 (2008) 192–201.
[12] P.S. Rao, I. Sen, Robust tuning of power system stabilizers using QFT, IEEE Trans. Control Syst. Technol. 7 (4) (1999) 478–486.
[13] P.S. Rao, I. Sen, Robust pole placement stabilizer design using linear matrix inequalities, IEEE Trans. Power Syst. 15 (February (1)) (2000) 313–319.
[14] H. Werner, P. Korba, T. Chen Yang, Robust tuning of power system stabilizers using LMI techniques, IEEE Trans. Control Syst. Technol. 11 (January (1)) (2003) 147–2003.
[15] M. Soliman, A.L. Elshafei, F. Bendary, W. Mansour, Robust decentralized PID-based power system stabilizer design using an ILMI approach, Electr. Power Syst. Res. 80 (December (12)) (2010) 1488–1497.
[16] M. Soliman, Characterization of all robust PD-based PSSs: an interval arithmetic approach, in: Proc. IEEE/PES General Meeting, Vancouver, BC, Canada, 21–23 July, 2013, pp. 1–5.
[17] E. Khutoryansky, M.A. Pai, Parametric robust stability of power systems using generalized Kharitonov's theorem, in: Proc. 36th Conference on Decision & Control, San Diego, California, December, 1997, pp. 3097–3099.
[18] H.M. Soliman, A.L. Elshafei, A. Shaltout, M.F. Morsi, Robust power system stabilizer, IEE Proc. Gen. Transm. Distrib. 147 (September (5)) (2000) 285–291.
[19] G. Rigatos, P. Saino, Design of robust electric power system stabilizers using Kharitonov's theorem, Math. Comp. Simul. 82 (2011) 181–191.
[20] H.M. Soliman, E.H. Bayaoumi, M.A. Awadallah, Reconfigurable fault tolerant PSS and FACTs controllers, Electr. Power Comp. Syst. 38 (2010) 1446–1468.
[21] Y.L. Abdel-Magid, M.A. Abido, Optimal multiobjective design of robust power system stabilizers using genetic algorithms, IEEE Trans. Power Syst. 18 (August (3)) (2003) 1125–1132.
[22] M.A. Abido, Particle swarm optimization for multimachine power system stabilizer design IEEE/PES, Summer Meeting, 15–19 July, vol. 3, 2001, pp. 1346–1351.
[23] V.L. Kharitonov, Asymptotic stability of an equilibrium position of a family of systems of linear differential equations, Differential'nye Uravnenya 14 (11) (1978) 2086–2088.
[24] B.R. Barmish, New Tools for Robustness of Linear Systems, MacMillan, New York, NY, 1994.
[25] A.C. Bartlett, C.V. Hollot, L. Huang, Root location of an entire polytope of polynomials: it suffices to check the edges, Math. Control Signals Syst. 1 (1) (1988) 61–71.
[26] S. Bialas, A necessary and sufficient condition for the stability of interval matrices, Int. J. Control 37 (4) (1983) 717–772.
[27] S.P. Bhatacharyya, H. Chapellat, L.H. Keel, Robust Control: The Parametric Approach, Prentice-Hall Inf.&Sys. Science, Har/Dis Edition, 1995.
[28] Hydro-Québec, TEQSIM International, Power System Blockset for Use with Simulink, User's Guide, The Math Works, Natick, MA, 1998.
[29] IEEE Power Engineering Society, IEEE Recommended Practice for Excitation System Models for Power System Stability Studies, IEEE Std 421.5™-2005, 2006.
[30] D.H. Baker, P.C. Krause, P.A. Rusche, An investigation of excitation system interaction, IEEE Trans. Power Appar. Syst. PAS-94 (3) (1975) 705–714.